VIROLOGY 193, 234–241 (1993)

Preliminary X-Ray Data Analysis of Crystalline Cowpea Chlorotic Mottle Virus

J. A. SPEIR, S. MUNSHI, T. S. BAKER, AND J. E. JOHNSON[1]

Department of Biological Sciences, Purdue University, West Lafayette, Indiana 47907

Received September 9, 1992; accepted October 30, 1992

Crystals of cowpea chlorotic mottle virus (CCMV) that diffract X-rays to 3.1 Å resolution were grown in a succinate–PEG solution buffered at pH 3.3. The crystals are in space group $P2_12_12_1$ with unit cell dimensions of a = 381.26 Å, b = 381.26 Å, and c = 408.59 Å. Four particles occupy the unit cell, placing a single virion in the crystallographic asymmetric unit. Diffraction intensities measured from 196 films collected at the Cornell High Energy Synchrotron Source accounted for 55% of the theoretically possible data to 3.2 Å. Unit cell dimensions and rotation function analyses of the X-ray data revealed that the particles were organized in a pseudo-tetragonal relationship with the pseudo-fourfold axis along the crystal c axis. Analysis of electron micrographs of two-dimensional crystals of CCMV revealed a remarkable similarity between these and planes of particles perpendicular to the crystallographic c axis in the three-dimensional crystal.

INTRODUCTION

Cowpea chlorotic mottle virus (CCMV) is a small RNA plant virus belonging to the bromovirus group of the proposed tricornavirus supergroup. Tripartite genomes encapsulated in polyhedral or bacilliform particles distinguish tricornaviruses from other plant virus taxa. The CCMV genome consists of three unique, single-stranded, positive-sense RNA molecules of 1.1×10^6 D (RNA 1), 1.0×10^6 D (RNA 2), and 0.75×10^6 D (RNA 3). RNA 1 and RNA 2 are encapsidated separately. RNA 3 is packaged along with a 0.35×10^6 D subgenomic RNA (RNA 4) into the same particle (Lane, 1974). The particle shell is composed of 180 identical protein subunits (19,800 MW; 189 aa) which form a 260-Å-diameter icosahedral shell with $T = 3$ quasi-symmetry (Caspar and Klug, 1962; Steven *et al.*, 1978; Dasgupta and Kaesberg, 1982).

CCMV is stable below pH 6.5; however, the virions undergo structural changes with variations in pH, temperature, and ionic strength (Bancroft *et al.*, 1967; Lane, 1974; Jacrot, 1975; Vriend *et al.*, 1982). Study of these structural transitions led to the first *in vitro* reassembly of a spherical virus from isolated CCMV protein and RNA (Bancroft *et al.*, 1967; Bancroft and Hiebert, 1967). CCMV particles are disrupted in high-ionic-strength solution ($I > 0.4$) at pH 7.5 in the absence of divalent metal ions. In the absence of salts and divalent metal ions, the particles maintain an increased or swollen hydrodynamic volume at pH ≥ 7.5. Swollen virus is sensitive to ribonuclease degradation which disrupts particles. Prior addition of 0.01 *M* $MgCl_2$ prevents swelling of CCMV under alkaline conditions and protects the viral RNA from ribonucleases, but does not prevent disruption of the particles at high ionic strength (Bancroft *et al.*, 1968). Purified, disassembled virus protein will assemble into empty protein capsids similar to the native virions when the pH is lowered to 5.0 in the presence of 100 m*M* NaCl (Bancroft *et al.*, 1969). These data describe a virus stabilized by protein–RNA interactions and pH-dependent divalent metal ion-mediated protein–protein interactions. Similar results have been observed for the type member of the bromovirus group, brome mosaic virus (BMV) (Pfeiffer and Hirth, 1974, 1975; Bancroft *et al.*, 1969). Studies of the reversible association and disassociation properties of bromovirus capsid proteins have been reviewed (Bancroft, 1970; Lane, 1974).

CCMV and BMV share extensive sequence homology between their tripartite genomes (Allison *et al.*, 1989), but heterologous combinations of RNAs 1 and 2 from each bromovirus do not support viral RNA replication (Traynor and Ahlquist, 1990). The availability of infectious cDNA clones for *in vitro* genetic manipulation of each virus (Allison *et al.*, 1988; Janda *et al.*, 1987) has made the bromovirus group an important system for studying positive-strand RNA virus replication (Ahlquist, 1992). Genomic RNAs 1 and 2 are monocistronic mRNAs encoding nonstructural proteins 1a and 2a, respectively. Both RNAs 1 and 2 are required for replication. RNA 3 is dispensable for bromovirus RNA replication *in vivo*, but encodes noncapsid protein 3a and the single capsid protein which are responsible for systemic movement of virus infection (Ahlquist, 1992). RNA 4 is a subgenomic monocistronic mRNA of

[1] To whom correspondence and reprint requests should be addressed.

0042-6822/93 $5.00

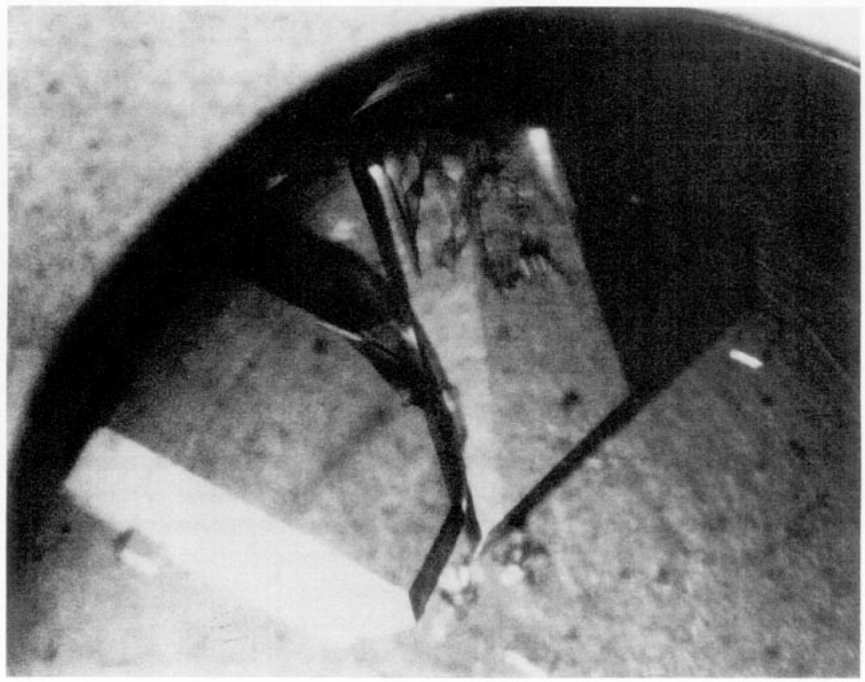

FIG. 1. Light photomicrograph of CCMV crystals (1.5 × 1.2 × 0.7 mm) grown in succinate-buffered polyethylene glycol solution at pH 3.3. The crystals grow in 3 to 5 days and diffract synchrotron radiation to 3.1 Å.

RNA 3 which expresses the coat protein gene separately. The function of the putative RNA binding region of the BMV coat protein N-terminus has been examined with deletion mutants (Sacher and Ahlquist, 1989). Removal of 25 amino acids of the N-terminal basic region completely abolished any signs of systemic infection. Deletion of the first 7 N-terminal amino acids left the basic region intact and did not hinder infection. In this mutant, infection spreads at normal speed, showing RNA packaging and symptoms of native virus infections. Mutational analysis and genetic exchanges between related BMV and CCMV RNA regions have been used to explore template specificity and other aspects of RNA replication used by each bromovirus. However, rational design of bromovirus protein capsid mutations has been limited due to the absence of a three-dimensional structure.

Poor diffraction of X-rays from previously studied CCMV single crystals (Rossmann *et al.*, 1973; Rayment *et al.*, 1977; Huess *et al.*, 1981) hindered a capsid structure determination to atomic resolution. This study reports successful collection of X-ray diffraction data for CCMV to 3.2 Å resolution. Crystals diffracting X-rays to high resolution were produced, in part, due to the elimination of ultracentrifugation-induced heterogeneity during purification of the virus. Crystals grown with virus unpelleted by ultracentrifugation consistently diffracted better than crystals produced with virus purified by published procedures. Preliminary data analysis revealed pseudo-tetragonal symmetry perpendicular to the crystal $\langle hk0 \rangle$ plane. Discovery of a two-dimensional crystalline array of CCMV with near identical pseudo-symmetry normal to the plane of the array (Baker, 1978) facilitated crystal packing analysis. This report details the first high-resolution X-ray data analysis for CCMV.

MATERIALS AND METHODS

Virus purification

CCMV was propagated in cowpea plants (*Vigna unguiculata* (L.) var. California Blackeye) and purified according to methods reported by Bancroft and Flack (1972) and Verduin (1978). Modifications described below improved crystal quality. All purification steps were performed at 4°C.

Infected secondary cowpea leaves were frozen at −20°C, crushed, and placed into a Waring blender. The contents were blended for approximately 3 min in homogenization buffer (0.2 *M* sodium acetate, 0.2 *M* acetic acid, 0.01 *M* ascorbic acid, 0.01 *M* disodium EDTA, pH 4.8). The homogenate was expressed through two layers of cheesecloth, and the foam was removed. The emulsion was allowed to separate on ice for 1 hr before being subjected to low-speed centrifugation (20 min at 20,000*g*) to pellet leaf tissue. Virus in the clear, supernatant fluid was precipitated by addition of 10% (w/v) polyethylene glycol (PEG) MW 8000, followed by slow overnight mixing. The precipitate was pelleted by low-speed centrifugation and then resuspended in storage buffer (0.1 *M* sodium acetate, 0.1 *M* acetic acid, 1 m*M* disodium EDTA, 1 m*M* sodium azide, pH 4.8). The resuspension was cleared of undissolved material by means of low-speed centrifugation. The virus was precipitated a second time with 15%

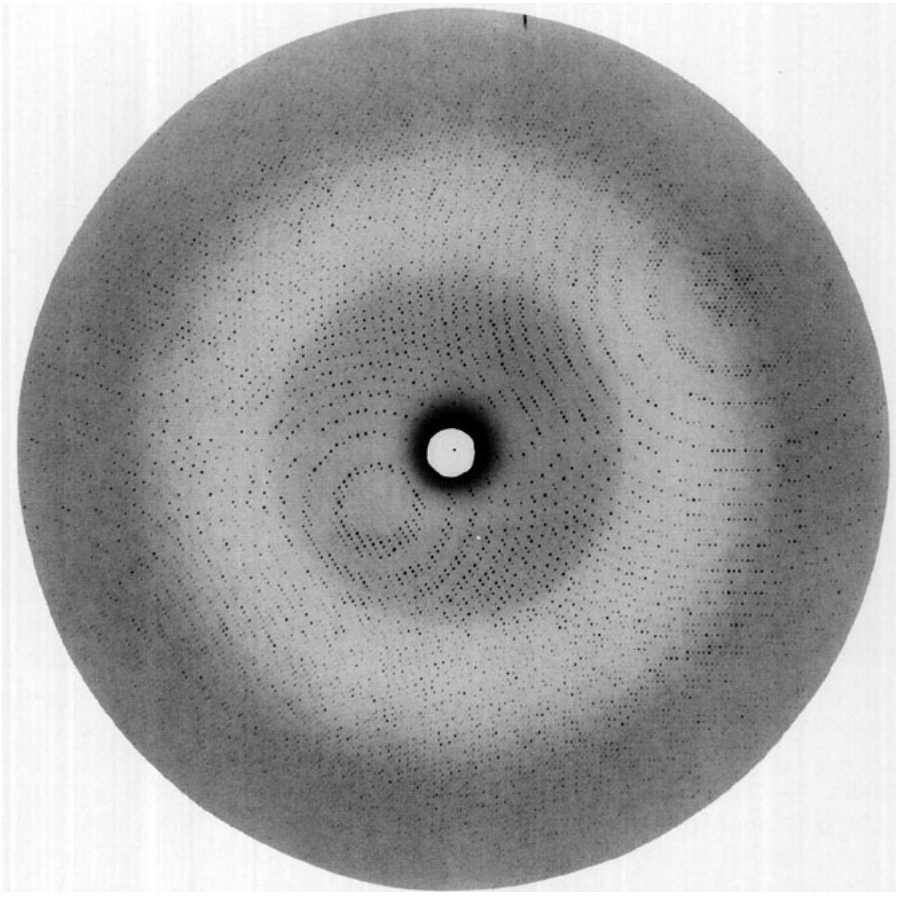

FIG. 2. A 0.3° oscillation photograph from a crystal of CCMV. The diffraction pattern was taken with the F-1 beam line at the Cornell High Energy Synchrotron Source. The wavelength was 0.910 Å, the crystal to film distance was 210.0 mm, and the exposure time was 36 sec. Data were measured to 3.3 Å resolution (the resolution limit at the edge of this photograph) with an average $F^2/\sigma(F^2)$ of 6.4 for data measured between 3.4 and 3.3 Å. Of the predicted 4349 whole and 18,024 partial reflections, 2703 whole and 8344 partial reflections were measured with $F^2/\sigma(F^2) \geq 2$.

(w/v) PEG MW 8000. The second virus resuspension was subjected to isopycnic ultracentrifugation in a solution of storage buffer brought to 38% (w/w) in CsCl. The virus band was dialyzed against three volume changes of storage buffer. Dialyzed virus solution was concentrated in Centricon 100 microconcentrators and then stored at 4°C in storage buffer. Typical yields were 200–300 mg of CCMV/kg of cowpea tissue.

Virus purity was determined by denaturing polyacrylamide gel electrophoresis of protein and by uv spectrophotometry ($E_{260}^{1\ mg/ml} = 5.87$; $A_{260}/A_{280} = 1.7$). The homogeneity of purified virus samples was tested by monitoring the uv absorbance distribution of small sample loads of CCMV (1 to 2 optical density units) separated on CsCl and sucrose gradients by isopycnic and rate zonal centrifugation, respectively. The structure and uniformity of purified virus particles were examined in an electron microscope.

Crystal growth and characterization

CCMV was crystallized by the sitting drop vapor diffusion method (McPherson, 1982). The reservoir buffer was 0.3 *M* disodium succinate, 0.3 *M* succinic acid, 1 m*M* sodium azide, 3.7–4.0% (w/v) PEG MW 8000, pH 3.3. Each droplet consisted of 5–25 μl of CCMV at 20–50 mg/ml in storage buffer, added to an equal volume of reservoir buffer. The dishes were sealed and allowed to equilibrate at room temperature in darkness against 15 ml of reservoir buffer.

Single crystals were examined with Cu$K\alpha$ radiation produced by an Elliot GX-20 rotating anode X-ray generator. Crystal diffraction quality was established by 3 hr still photography. Screenless, zero-layer precession photographs ($\mu = 1.5°$, 29 Å resolution) of the principal zones provided an approximate measure of the unit cell constants and a determination of the space group.

Data collection, processing, and rotation function analysis

Data were collected on film by oscillation photography (oscillation angles of 0.3° and 0.4°) at the Cornell High Energy Synchrotron Source (CHESS) ($\lambda = 0.910$ Å with crystal to film distances of 189.7 and 210.0 mm; λ

TABLE 1

A SUMMARY OF REFLECTIONS MEASURED AFTER SCALING OF 196 OSCILLATION FILMS FROM 70 CRYSTALS[a]

Resolution (Å)	Number of unique reflections	Percentage of theoretically observable data
30–25	695	83
25–15	6,435	89
15–10	19,395	89
10–8	26,206	88
8–6	68,390	82
6–5	81,741	78
5–4	164,503	69
4–3.5	109,960	46
3.5–3.2	44,441	20
Totals: 30–3.2	521,766	55

[a] The CCMV space group was determined to be $P2_12_12_1$ with a = 381.26 Å, b = 381.26 Å, and c = 408.59 Å. The scaling R factor for whole reflections and partial reflections with a partiality greater than 0.25 was 12.53%. The data consisted of 1,014,619 observations (521,766 unique reflections) with $F^2/\sigma \geq 4$. The number of theoretically observable unique reflections to 3.2 Å is 954,874.

= 1.565 Å with a crystal to film distance of 100.0 mm). The oscillation films were scanned on an Optronics rotating drum photoscanner (System P-1000). The crystal orientation relative to the camera coordinate system was determined by an automatic indexing program developed by Kim (1989). Diffraction intensities were measured with the program developed by Rossmann (1979). The data were scaled and postrefined to achieve better estimates of reflection partiality, crystal setting, lattice parameters, and crystal mosaicity (Rossmann *et al.*, 1979). The self-rotation function (Rossmann and Blow, 1962) was computed to search for the direction of icosahedral noncrystallographic symmetry elements. To enhance the signal-to-noise ratio in the absence of a complete data set, a locked self-rotation function algorithm (Tong and Rossmann, 1990) was computed to search simultaneously for all noncrystallographic symmetry.

RESULTS

Crystal analysis

Orthorhombic crystals grew as large as 2.5 mm in 3 to 5 days (Fig. 1). The crystals exhibited prominent ⟨110⟩ faces and remained stable in vapor diffusion growth chambers at room temperature.

The crystals diffracted Cu$K\alpha$ X-rays to 3.3 Å resolution and synchrotron (CHESS) radiation to 3.1 Å resolution (Fig. 2), although crystals were sensitive to radiation from both sources. Crystal life times varied from 5 to 15 hr in the presence of Cu$K\alpha$ X-rays, thus making it difficult to obtain low-resolution precession photographs on rotating anode X-ray generators. Symmetry on precession photographs of the crystal ($hk0$) and (11ℓ) planes indicated an orthorhombic unit cell. Measurements gave approximate unit cell constants of a = b = 385 Å, and c = 399 Å. A volume per virus molecular weight (V_m; Mathews, 1968) value of 3.2 Å^3 D^{-1} indicated a total of four virus particles per unit cell. Systematic absences of odd reflections along the three unit cell axial directions indicated three perpendicular 2_1 screw axes.

The crystal sensitivity to CHESS radiation restricted the number of exposures that could be obtained from a single crystal. The crystal was translated after each photograph to record multiple exposures. The typical crystal life time was about 3 min, just enough to take two exposures. This prevented optimizing the crystal setting for data collection. The lattice dimensions measured from high-resolution oscillation films suggested tetragonal lattice symmetry. Ten films were indexed, resulting in an average value of 382 ± 1.0 Å for the a and b cell dimensions. The small deviation of 1.0 Å suggested that the lattice may have a fourfold axis coincident with the c axis, although this was not apparent on precession photographs. Attempts were made to index the lattice as 4mm and to measure symmetry-related diffraction intensities. Films processed in this manner gave ≥40% R factors[2] for symmetry-related reflections found on single films. Indexed as mmm, the same films gave 15% or lower R factors for symmetry-related reflections. Analysis of $h00$, $0k0$, and 00ℓ diffraction intensities from these measurements revealed near zero or negative values for the odd reflections to 3.2 Å resolution. Data measured from precession films and oscillation films indexed as mmm were consistent with the $P2_12_12_1$ space group.

Data processing

Diffraction intensities were measured from 196 films. B-films were processed for 138 of the 196 films. A-film/B-film pairs were scaled to allow more accurate measurement of low-resolution reflections. Photographs collected with a 0.4° oscillation angle contained substantial reflection overlap which limited intensity measurement to 4 Å resolution. An oscillation angle of 0.3° resulted in fewer overlaps and allowed diffraction intensities to be measured to 3.2 Å resolution. Individual film data were combined and scaled, but unreasonably high R factors were obtained for symmetry-related reflections measured from exposures of the same crystal. Examination of the crystal orientation matrices for each film revealed that the orthorhombic lattice was indexed in two distinct orientations. Films from the same crystal were indexed as

[2] R factor = $[\Sigma_h\Sigma_i(I_h - I_{hi})/\Sigma_h\Sigma_i I_{hi}] \times 100$, where I_h is the mean of the I_{hi} observations of reflection h.

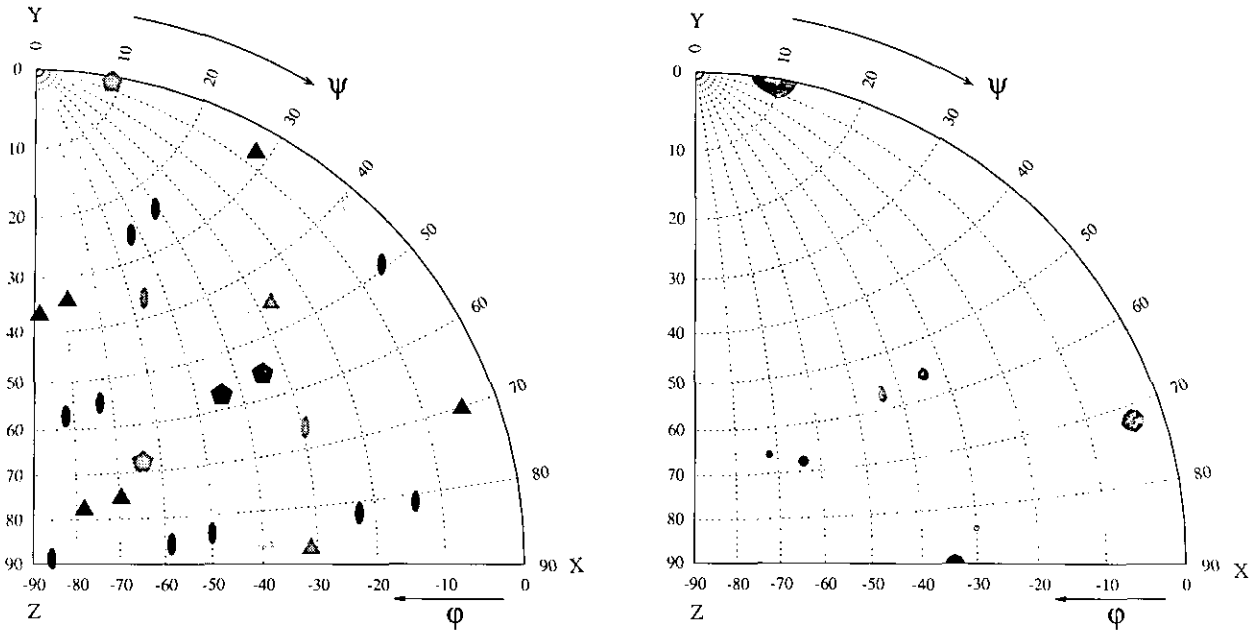

FIG. 3. Comparison of results from the $\kappa = 72°$ self-rotation function (right plot) and locked self-rotation function (left plot). Both stereographic plots represent identically oriented crystallographic asymmetric units where rotation function *X*, *Y*, and *Z* axes are coincident with the crystallographic *a*, *b*, and *c* axes, respectively. The *Z* axis projects out of the page. The standard icosahedron orientation for both searches was, going from *X* to *Z*, twofold axis–threefold axis–fivefold axis–twofold axis. Rotation function analysis determined that symmetry elements of the icosahedron in the standard orientation are oriented in the crystal cell by the following operations: $X_{\text{crystal}} = [\rho]X_{\text{standard orthogonal}}$, where ρ is a matrix to rotate coordinates within the orthogonal system,

$$[\rho] = \begin{bmatrix} 0.1160 & -0.9594 & 0.2570 \\ 0.5431 & -0.1554 & -0.8252 \\ 0.8316 & 0.2353 & 0.5030 \end{bmatrix}$$

The self-rotation function was computed with $\kappa = 72°$ in 2° increments of ϕ and ψ, and included 76,088 reflections (67.2% of the data) measured between 7.5 and 5.5 Å resolution. 1042 large terms ($I > 4 \times I_{av}$, 1.37% of the data) were used in the rotated Patterson, and the radius of integration was 175 Å. Contour lines were drawn in 0.5σ increments from a minimum of 3.5σ to a maximum of 9.5σ, where σ is the standard deviation for this rotation function. The locked self-rotation function was computed over 10° intervals for data between 15 and 8.5 Å resolution and with a radius of integration of 130 Å. The solution was identified as a 4.4σ peak and determined to higher precision with a 0.1° fine search. The symbols were shaded in four levels corresponding to the four sets of icosahedral symmetry operators oriented relative to the crystal axes. Symbols with the same shading correspond to the same virus particle. Fivefold, threefold, and twofold rotation axes are depicted with pentagons, triangles, and ovals, respectively. Comparison of the directions of fivefold icosahedral axes between the two searches revealed precise agreement between their locations. Note that pentagon symbols of all four shades match with contours in the right plot, demonstrating the four particle orientations which produced the numerous fivefold peaks in the self-rotation function; however the peak at $\phi = -34°$, $\psi = 0°$ is not a part of icosahedral symmetry.

either of two nearly identical lattices, due to identical *a* and *b* lattice dimensions. One of the lattices was arbitrarily chosen as a reference. Nonstandard lattice assignments, which were identified by scaling statistics, were converted to standard assignments. Reflections with $F^2/\sigma(F^2) \geq 4$ from the 196 films scaled together with an *R* factor of 12.5%. Postrefinement of the data resulted in convergence of the lattice constants to $a = b = 381.26$ Å, and $c = 408.59$ Å. Table 1 summarizes the data collection as a function of resolution.

Rotation function

The rotation function determines the orientation of noncrystallographic symmetry elements relative to the crystal axes (Rossmann and Blow, 1962). The correct CCMV particle orientation is required for precise placement of a suitable model into the CCMV unit cell to compute initial phases for molecular replacement and to average electron density over the icosahedral noncrystallographic symmetry. Each of the four CCMV virions occupies one crystallographic asymmetric unit, allowing the entire symmetry of the icosahedral point group to be used for real space phase refinement. Self-rotation function analysis revealed more than the 31 symmetry positions (15 twofold axes, 10 threefold axes, and 6 fivefold axes) required to define the orientation of a single CCMV particle. This result showed that the particles were in a general orientation relative to the crystallographic axes. The locked self-rotation function searches for all icosahedral noncrystallographic symmetry simultaneously, allowing the R_L

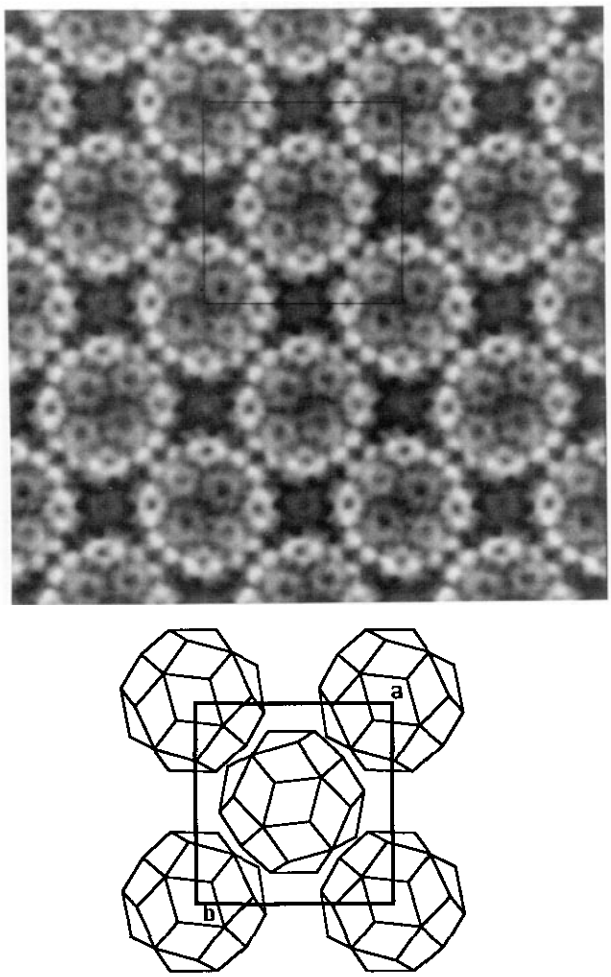

FIG. 4. Comparison of CCMV particle packing in a two-dimensional crystalline array and a three-dimensional crystal. (Top) A computer-filtered image of a two-dimensional crystalline array of negatively stained CCMV. One unit cell is outlined. Neighboring viruses in the array are related by a 94°/86° rotation, creating a pseudo-tetragonal axis normal to the plane of the array. The lattice constants for the array ($a = b = 375$ Å) are similar to two of the lattice constants for the three-dimensional CCMV crystals ($a = b = 381.26$ Å). (Bottom) Diagram showing particles in the a–b plane of the three-dimensional crystal. The unit cell is outlined as for the two-dimensional array above. The virus particles are represented by rhombic triicontahedrons. Nearest neighbor viruses in the crystal a–b planes are related by a 99°/81° rotation. The near identical lattice dimensions, screw axis symmetry, and pseudo-tetragonal symmetry in the two types of crystalline samples suggested that the two-dimensional array corresponds to an a–b plane of the three-dimensional crystal.

function[3] *to be averaged at each point in the search.* The locked self-rotation function can be interpreted as a search for only a single particle orientation at each point of the search, and this was used to identify the symmetry elements consistent with each particle in the unit cell (Fig. 3). A single locked self-rotation function solution was identified. Generation of the three crystallographically related particle orientations confirmed that four orientations existed relative to the crystal lattice. The location of the four sets of icosahedral symmetry operators determined by the locked self-rotation function gave precise correlations to the peaks found in the self-rotation function searches (Fig. 3). All 124 (31 symmetry operators per particle × 4 particles per unit cell) noncrystallographic symmetry operators were clearly identified.

[3] $R_L = (\Sigma_i R/n)$, where R_L is the averaged sum over the n symmetry operators R_i of the input point group.

Virion packing

The rotation function solution was consistent with particle orientations found in a two-dimensional crystalline array of CCMV (Baker, 1978; Fig. 4). Electron microscopy and image analysis revealed pseudo-tetragonal symmetry normal to the plane of the array. The orientation of the pseudo-symmetry axis in the array was equivalent to the orientation of the pseudo-tetragonal crystal c axis. Visually, the array appeared to be $P42_12$, but quantitative image analysis showed the lattice to be $P2_12_12$ with $a = b = 375$ Å. The particles in the array could be superimposed by a 94°/86° rotation *about the normal to the array. The rotation function* results determined that particles in the crystal could be superimposed by a rotation of 99°/81° about the crystal c axis. The similarity in lattice parameters and pseudo-tetragonal character between the two-dimensional array and the three-dimensional crystal facilitated building of a packing model for the CCMV unit cell (Fig. 5). The packing model suggested positions for CCMV at either (0, 0, 0) or (0.25, 0.25, 0.25). Packing analysis with 280-Å-diameter model spheres revealed

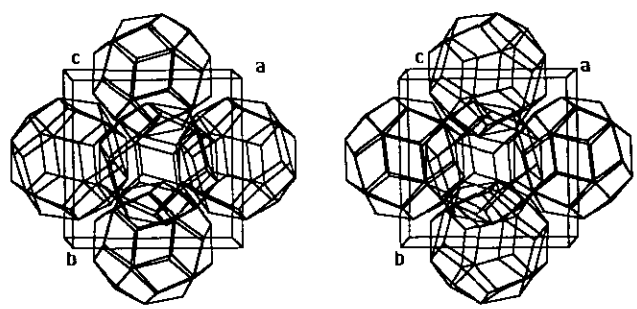

FIG. 5. Stereo pair diagram of the proposed $P2_12_12_1$ crystal packing of CCMV particles. The unit cell axes are labeled with the crystal *c axis (pseudo-tetragonal axis) projecting out of the page. The virus* particles, represented by 280-Å-diameter rhombic triicontahedrons, are oriented as in the crystal and placed with one molecular center at (0, 0, 0). The particle twofold axes are nearly parallel to the crystal c axis. With the array in Fig. 4 assumed to be a crystal a–b plane, this three-dimensional packing model was built by stacking these a–b layers perpendicular to c, such that large holes in one layer become *filled with virus particles in adjoining layers. This model obeys the* $P2_12_12_1$ space group symmetry and has four virus particle orientations relative to the crystal lattice. Interparticle center-to-center distances within ($hk0$) and between (11ℓ) layers agree well with the particle dimensions determined by electron microscopy.

that these positions were sterically equivalent and at the center of a uniform packing environment created by 12 neighboring particles. A small deviation from (0, 0, 0) or (0.25, 0.25, 0.25) eliminated the uniform 12-particle packing environment at each position. No other positions had packing environments of this nature.

DISCUSSION

The difficulties in growing CCMV crystals which diffract X-rays to high resolution were overcome. The most significant difference from past CCMV crystal diffraction studies is found in the purification protocol. Crystals of CCMV originally grown in our laboratory involved use of virus that was pelleted by means of high-velocity centrifugation. Crystals grown from such virus only diffracted X-rays to 3.6 Å resolution. Changing the purification strategy (not the crystallization conditions) appeared to be the primary factor which increased crystal diffraction ability to 3.1 Å resolution.

Knowledge of the structure of CCMV will lead to a better understanding of the complex assembly properties of spherical plant viruses. Visualization of coat protein contacts may reveal how pH and divalent cations affect the stability of native and swollen CCMV capsids. Correlation of this structural information to the extensive literature on bromovirus biophysical, biochemical, and molecular biological properties should lead to a better understanding of the biology of bromoviruses.

Phasing attempts by the molecular replacement technique have been initiated. The southern bean mosaic virus (SBMV; Silva and Rossmann, 1987) model was modified to fit the reconstructed density determined from recently obtained cryo-electron microscopy images of CCMV at 20 Å resolution (Wang *et al.*, 1993). The modified SBMV model was oriented and placed into the CCMV unit cell to calculate an initial set of phases for the CCMV amplitudes.

ACKNOWLEDGMENTS

We thank Dr. Paul Ahlquist for supplying infectious CCMV for propagation, Andrew Fisher for assistance in preparing Figs. 4 and 5, and Cindy Music for photographic assistance in preparing Fig. 4. We also thank the staff at CHESS and members of the JEJ laboratory for assistance in data collection. This work was supported by National Science Foundation Grant 8817057A1-DMB to J.E.J., National Science Foundation Grant 8905062-DMB to T.S.B., and a grant from the Lucille P. Markey Foundation. J.A.S. was supported by National Institutes of Health Biophysics Training Grant GM08296.

REFERENCES

ALLISON, R. F., JANDA, M., and AHLQUIST, P. (1988). Infectious *in vitro* transcripts form cowpea chlorotic mottle virus cDNA clones and exchange of individual RNA components with brome mosaic virus. *J. Gen. Virol.* **62,** 3581–3588.

ALLISON, R., JANDA, M., and AHLQUIST, P. (1989). Sequence of cowpea chlorotic mottle virus RNAs 2 and 3, and evidence of a recombination event during bromoviral evolution. *Virology* **172,** 321–330.

AHLQUIST, P. (1992). Bromovirus RNA replication and transcription. *Curr. Opinion Genet. Dev.* **2,** 71–76.

BAKER, T. S. (1978). The packing of cowpea chlorotic mottle virus in crystalline monolayers. *Ninth Intl. Congress on Electron Microscopy* **2,** 24–25.

BANCROFT, J. B. (1970). The self-assembly of spherical plant viruses. *Adv. Virus Res.* **16,** 99–134.

BANCROFT, J. B., BRACKER, C. E., and WAGNER, G. W. (1969). Structures derived from cowpea chlorotic mottle and brome mosaic virus protein. *Virology* **38,** 324–335.

BANCROFT, J. B., and FLACK, I. H. (1972). The behavior of cowpea chlorotic mottle virus in CsCl. *J. Gen. Virol.* **15,** 247–251.

BANCROFT, J. B., HIEBERT, E., REES, M. W., and MARKHAM, R. (1968). Properties of cowpea chlorotic mottle virus, its protein and nucleic acid. *Virology* **34,** 224–239.

BANCROFT, J. B., and HIEBERT, E. (1967). Formation of an infectious nucleoprotein from protein and nucleic acid isolated from a small spherical virus. *Virology* **32,** 354–356.

BANCROFT, J. B., HILLS, G. J., and MARKHAM, R. (1967). A study of the self-assembly process in a small spherical virus: formation of organized structures from protein subunits *in vitro*. *Virology* **31,** 354–379.

CASPAR, D. L. D., and KLUG, A. (1962). Physical principles in the construction of regular viruses. *Cold Spring Harbor Symp. Quant. Biol.* **27,** 1–24.

DASGUPTA, R., and KAESBERG, P. (1982). Complete nucleotide sequences of the coat protein messenger RNAs of brome mosaic virus and cowpea chlorotic mottle virus. *Nucleic Acids Res.* **10,** 703–713.

HUESS, K. L., RAO, J. K., and ARGOS, P. (1981). Crystallization of cowpea chlorotic mottle virus. *J. Mol. Biol.* **146,** 635–640.

JACROT, B. (1975). Studies on the assembly of a spherical virus. II. The mechanism of protein aggregation and virus swelling. *J. Mol. Biol.* **95,** 433–446.

JANDA, M., FRENCH, R., and AHLQUIST, P. (1987). High efficiency T7 polymerase synthesis of infectious RNA from cloned brome mosaic virus cDNA and effects of 5′ extensions on transcript infectivity. *Virology* **158,** 259–262.

KIM, S. (1989). Auto-indexing oscillation photographs. *J. Appl. Crystallogr.* **22,** 53–60.

LANE, L. C. (1974). The bromoviruses. *Adv. Virus Res.* **19,** 151–220.

MATHEWS, B. W. (1968). Solvent content of protein crystals. *J. Mol. Biol.* **33,** 491–497.

MCPHERSON, A. (1982). "Preparation and Analysis of Protein Crystals." Wiley, New York.

PFEIFFER, P., and HIRTH, L. (1974). Formation of artificial top component from brome mosaic virus at high salt concentrations. *Virology* **58,** 362–368.

PFEIFFER, P., and HIRTH, L. (1975). The effect of conformational changes in brome mosaic virus upon its sensitivity to trypsin, chymotrypsin, and ribonuclease. *FEBS Lett.* **56,** 144–148.

RAYMENT, I., ARGOS, P., and JOHNSON, J. E. (1977). Crystalline cowpea chlorotic mottle virus. *J. Ultrastruct. Res.* **61,** 240–242.

ROSSMANN, M. G. (1979). Processing oscillation diffraction data for very large unit cells with an automatic convolution technique and profile fitting. *J. Appl. Crystallogr.* **12,** 570–581.

ROSSMANN, M. G., and BLOW, D. M. (1962). The detection of subunits within the crystallographic asymmetric unit. *Acta Crystallogr.* **15,** 24.

ROSSMANN, M. G., LESLIE, A. G. W., ABDEL-MEGID, S. S., and TSUKIHARA, T. (1979). Processing and post-refinement of oscillation camera data. *J. Appl. Crystallogr.* **12,** 570–581.

ROSSMANN, M. G., SMILEY, I. E., and WAGNER, M. A. (1973). Crystalline cowpea chlorotic mottle virus. *J. Mol. Biol.* **74,** 255–256.

SACHER, R., and AHLQUIST, P. (1989). Effects of deletions in the N-terminal basic arm of brome mosaic virus coat protein on RNA packaging and systemic infection. *J. Virol.* **63,** 4545–4552.

SILVA, A. M., and ROSSMANN, M. G. (1987). Refined structure of southern bean mosaic virus at 2.9 Å resolution. *J. Mol. Biol.* **197,** 69–87.

STEVEN, A. C., SMITH, P. R., and HORNE, R. W. (1978). Capsid fine structure of cowpea chlorotic mottle virus: From a computer analysis of negatively stained virus arrays. *J. Ultrastruct. Res.* **64,** 63–73.

TONG, L., and ROSSMANN, M. G. (1990). The locked rotation function. *Acta Crystallogr.* **A46,** 783–792.

TRAYNOR, P., and AHLQUIST, P. (1990). Use of bromovirus RNA2 hybrids to map *cis*- and *trans*-acting functions in a conserved RNA replication gene. *J. Virol.* **64,** 69–77.

WANG, G., SPEIR, J. A., FOX, J., CHENG, H., OLSON, N., YOUNG, M., BAKER, T. S. and JOHNSON, J. E. (1993). The structures of native, swollen, and empty particles of cowpea chlorotic mottle virus by cryo-electron microscopy and three-dimensional image analysis. Manuscript in preparation.

VERDUIN, B. J. M. (1978). Degradation of cowpea chlorotic mottle virus ribonucleic acid *in situ*. *J. Gen. Virol.* **39,** 131–147.

VRIEND, G., HEMMINGA, M. A., VERDUIN, B. J. M., and SCHAAFSMA, T. J. (1982). Swelling of cowpea chlorotic mottle virus studied by proton nuclear magnetic resonance. *FEBS Lett.* **146,** 319–321.